*Supporting Information for*

# Controlling Solid-Gas Reactions at Nanoscale for Enhanced Thin Film Morphologies and Device Performances in Solution-Processed $Cu_2ZnSn(S,Se)_4$ Solar Cells

Chengyang Jiang,[†‡] Yao-Tsung Hsieh,[†‡] Hongxiang Zhao,[†‡] Huanping Zhou,[†‡] and Yang Yang[*,†‡]

†Department of Materials Science and Engineering and ‡California NanoSystems Institute, University of California, Los Angeles, California 90095, United States

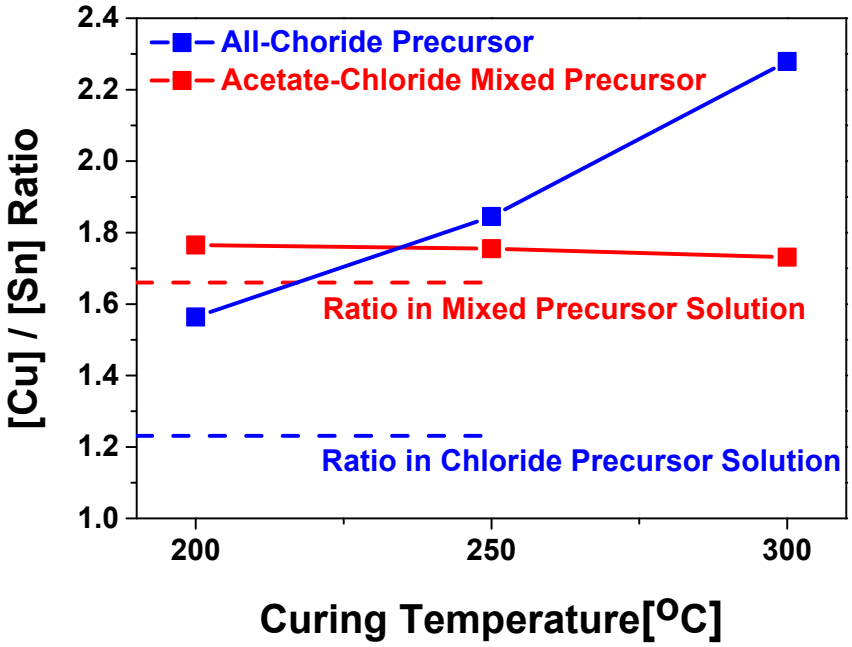


**Figure S1.** Influence of curing temperature on the copper to tin ratio in the precursor films. In all chloride precursors (blue line), the ratio in films deviates from that in the solution and changes significantly with varying curing temperature. As for acetate-chloride mixed precursor (red line), the ratio in films is comparable to that in the solution and almost remain constant as curing temperature varies.

**Figure S2.** The mixture of $Cu(OAc)_2$, $SnCl_2$, $Zn(OAc)_2$ and thiourea dispersed in various solvents: (left) MeOH; (middle) 1:1 mixture of EtOH and 2-ME; (right) 1:1 mixture of MeOH and 2-ME.

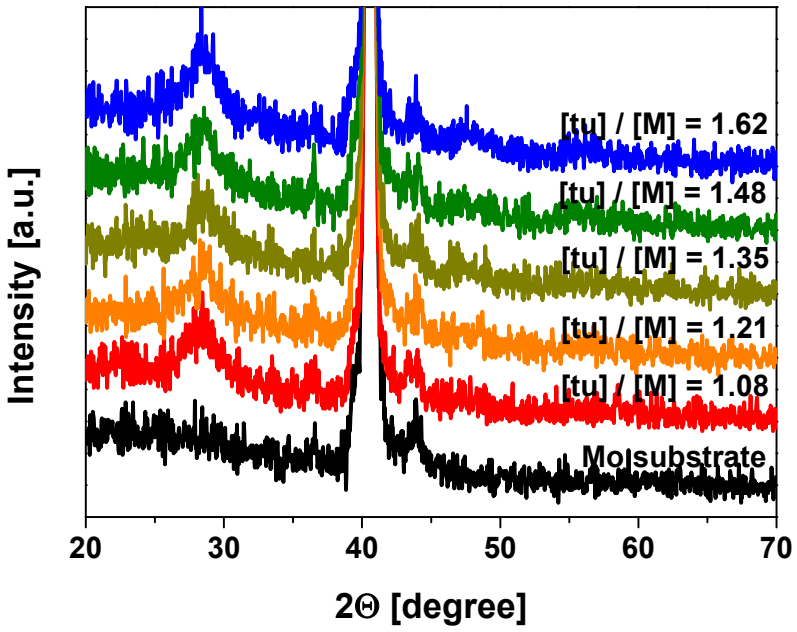


**Figure S3.** XRD patterns of CZTS NPs formed *in-situ* via sol-gel processes using different amount of thiourea. ([tu] = concentration of thiourea, [M] = concentration of total metal ions)

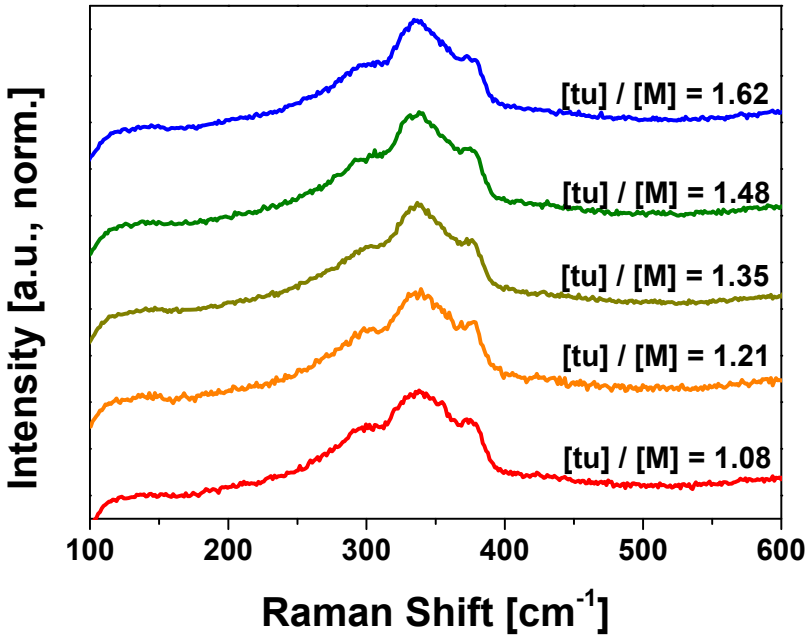


**Figure S4.** Raman spectra of CZTS NPs formed *in-situ* via sol-gel processes using different amount of thiourea.

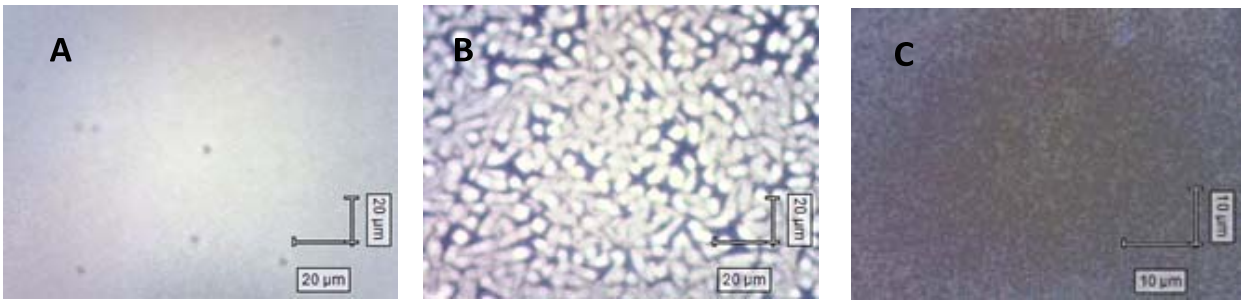


**Figure S5.** (A) Optical image of 700 nm precursor film deposited with only low temperature curing (refer to Experimental Section). (B) Optical image of 900 nm precursor film deposited with only low temperature curing. Cracks due to film stress can be clearly seen. (C) Optical image of 1100 nm precursor film deposited with high temperature curing. No cracks are seen because high-temperature curing increases grain sizes and film ductility, thus releasing stress.

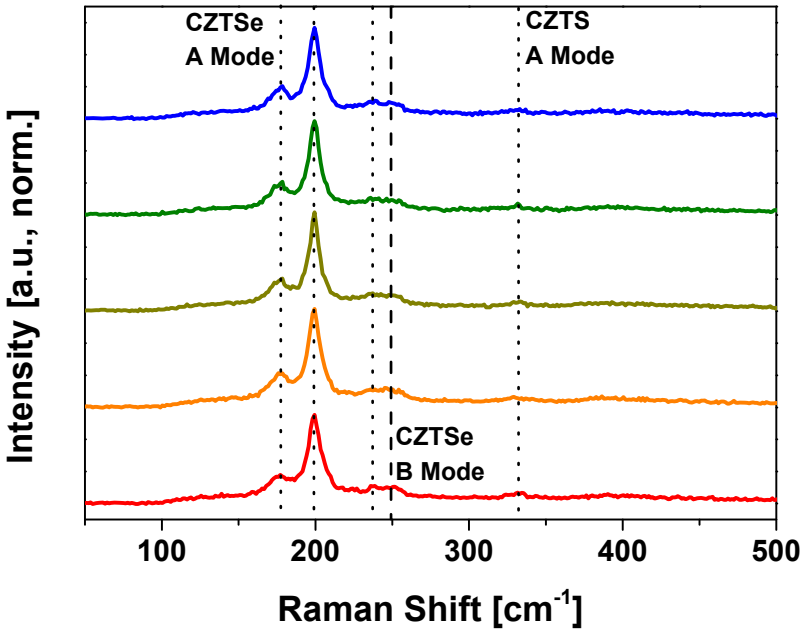


**Figure S6.** Raman spectra of selenized CZTSSe films from molecular inks with different amount of thiourea.

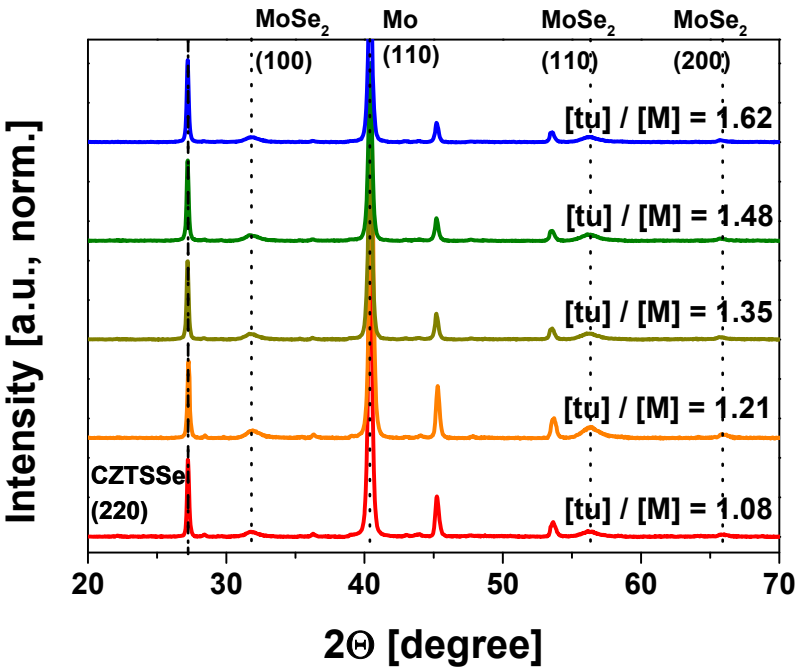


**Figure S7.** XRD patterns of selenized CZTSSe films from molecular inks with different amount of thiourea.

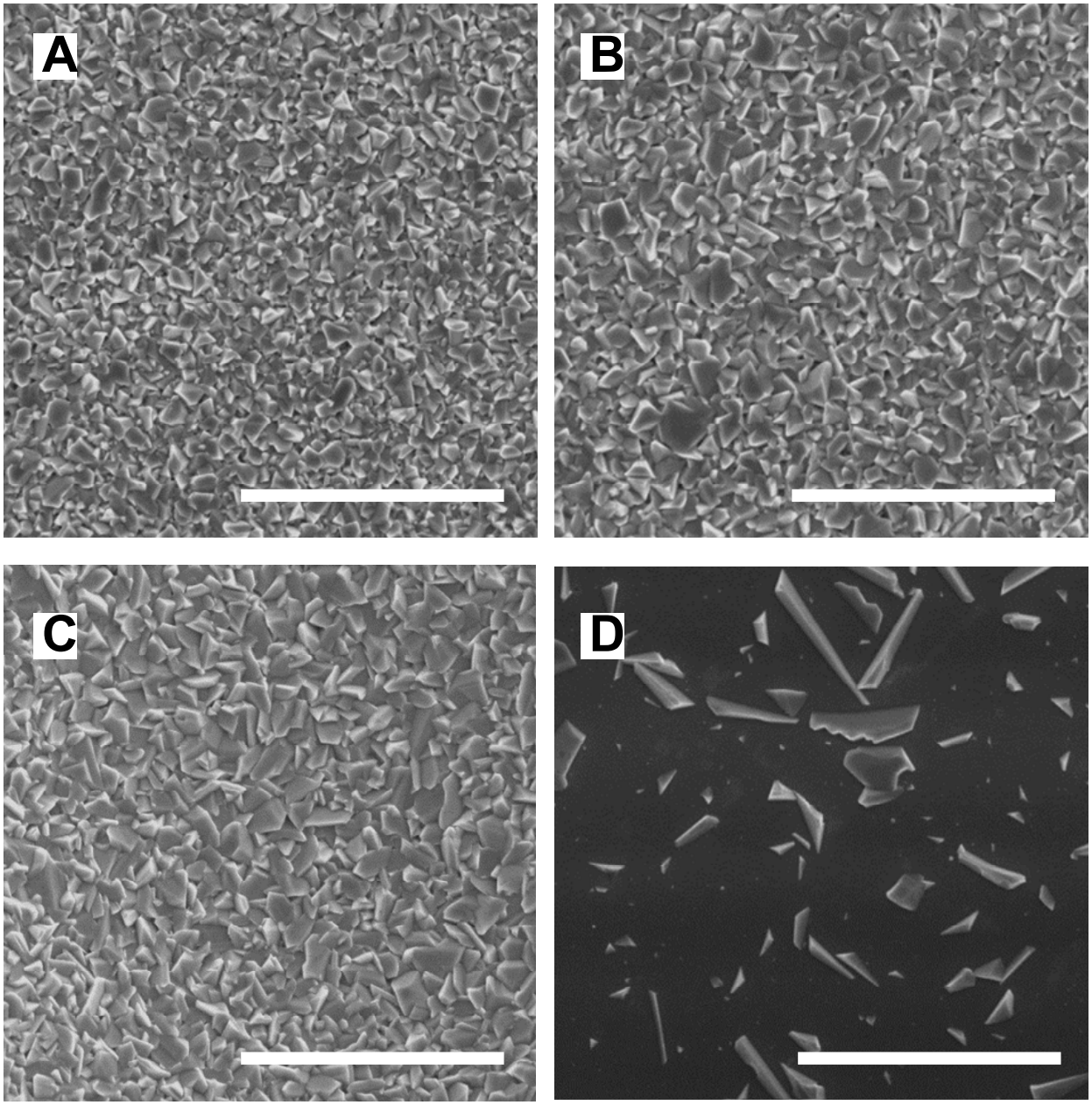


**Figure S8.** SEM images of CZTS films deposited using precursor inks with [tu]/[M] equal to (A) 1.08, (B) 1.21, (C) 1.35 or (D) 1.62, all selenized at 540°C for 15 min (scale bar = 5 μm).

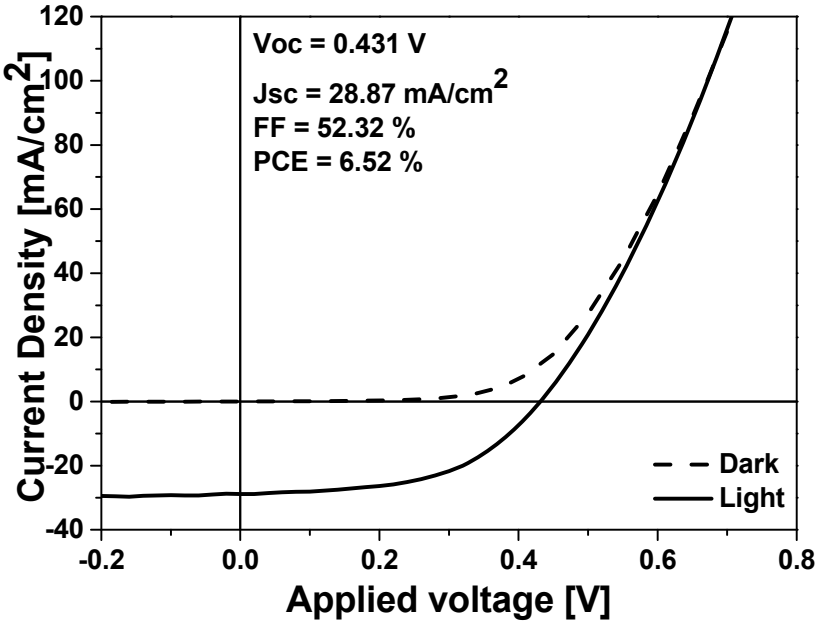


**Figure S9.** Device characteristics of the best-performing CZTSSe device ([tu] / [M] = 1.35).

| [tu]/[M] | $V_{OC}$ (V) | $J_{SC}$ (mA/cm$^2$) | FF (%) | PCE (%) |
|---|---|---|---|---|
| 1.08 | 0.407±0.007 | 22.14±0.51 | 47.78±2.79 | 4.31±0.37 |
| 1.21 | 0.419±0.006 | 23.97±0.67 | 46.10±3.36 | 4.64±0.52 |
| 1.35 | 0.410±0.011 | 26.38±3.44 | 47.61±4.67 | 5.12±0.65 |
| 1.48 | 0.306±0.013 | 14.65±2.17 | 33.36±5.26 | 1.52±0.43 |
| 1.62 | 0.067±0.024 | 4.79±2.62 | 24.39±1.91 | 0.09+0.10 |

**Table S1.** Average device characteristics of CZTSSe cells (12 cells for each [tu]/[M] ratio) with various amount of thiourea in the precursors. When [tu]/[M] ratio reaches 1.48 and 1.62, the relative standard deviations of all device characteristics become significantly larger, indicating sever morphological imhomogeneities.

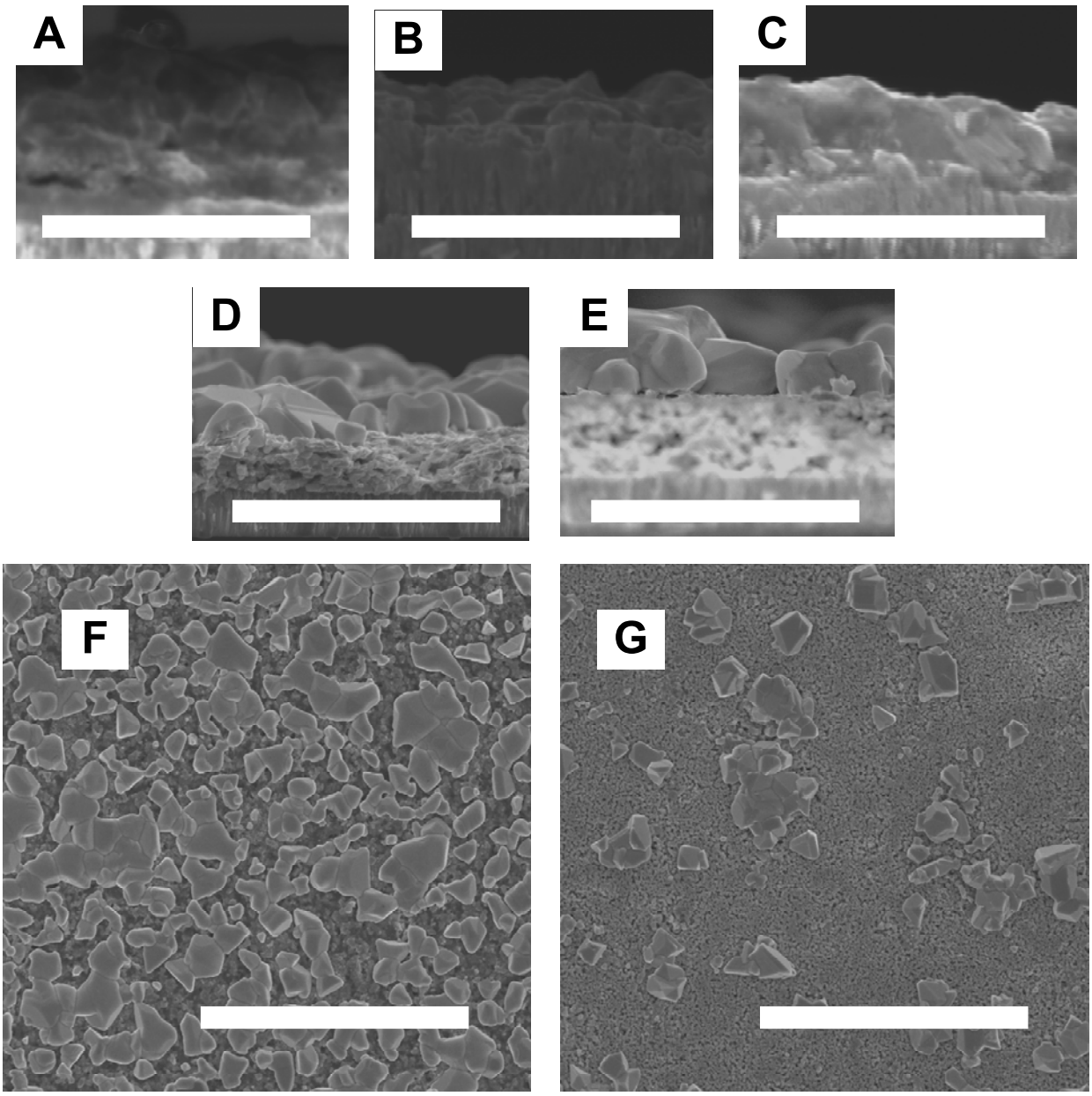


**Figure S10.** (A-E) Cross sectional SEM images of CZTSe thin films derived from precursors with [tu]/[M] equal to (A) 1.08, (B) 1.21, (C) 1.35, (D) 1.48 and (E) 1.62. (Scale bar = 2 μm.) (F-G) Plan view SEM images of same samples as for (D) and (E).